Journal of Hydroscience and Hydraulic Engineering
Vol. 27, No.2 November, 2009, 17-27

EVALUATION OF EVAPORATION FLUX UNDER QUASI-UNSTEADY WIND VELOCITY

By

Hiroaki Terasaki

Department of Architecture and Civil Engineering, University of Fukui, Bunkyo, Fukui, Japan

Teruyuki Fukuhara

Department of Architecture and Civil Engineering, University of Fukui, Bunkyo, Fukui, Japan

Koji Kadono

Criminal Investigation Laboratory, Shiga Prefectural Police, Ootsu, Shiga, Japan

and

Kazuro Nakane

Flood disaster investigation, National Research Institute for Earth Science and Disaster Prevention, Tsukuba, Ibaraki, Japan

SYNOPSIS

The present paper describes a new method to calculate the hourly evaporation flux under quasi-unsteady wind velocity using a wind tunnel that can supply a set of high and low speed winds with arbitrary time intervals. Soil columns filled with Chao soil and Toyoura standard sand were used in wind tunnel evaporation experiments. The hourly averaged free-stream velocity, V_{w0}^{ave}, had the same value for all wind velocity combinations. In spite of the same V_{w0}^{ave}, the difference in the cumulative evaporation at 150 hours after the beginning of the experiment became no less than 8-12% by changing the combinations of high and low speed winds, regardless of the soil. This is attributed to the nonlinear relation between the evaporation coefficient, α_v, and the free-stream velocity, V_{w0}. Findings show that the hourly evaporation flux calculated using two different α_v values for high and low wind velocties is more accurate than that calculated using α_v for V_{w0}^{ave}.

INTRODUCTION

The problem of evaporation is closely related to the preservation of water resources for drinking and irrigation water, soil hazards due to salt, heat islands, global warming, etc.

A lysimeter and an evaporation pan (a soil tank) are used to measure evaporation or evapotranspiration. The evaporation flux is obtained by calculating the decrease in the weight of the soil tank associated with evaporation over the time interval of the measurement. Saito et al. (1) found that a lysimeter tends to overestimate evapotranspiration for several days after rainfall, although there was no deterioration of the measuring system. Since a rule or a balance is used for the measurement of evaporation with an evaporation pan, automatic and sequential collection of data are difficult in the field. Much work is, therefore, necessary for long-term observations.

The eddy correlation method is also a widely used technique. In this method, evaporation is calculated from a direct measurement of turbulent transport and is useful to the diagnosis of the transport of the sensible heat, latent heat and CO_2 between the land (or sea) and the atmosphere (Tamagawa (2), Narimatsu et al. (3), Machimura (4), Iwata et al. (5)). This method requires, however, much maintenance and human work to carry out regular calibrations and to get adjustments of the hygrometer and the anemometer. Moreover, it is necessary to examined whether the vapor flux, calculated at a measurement point, fully represents evaporation from the ground or water surface under the measurement point.

On the other hand, the energy balance method is a common indirect method (Kondo (6), Kimura et al. (7)). Of course in this method the accuracy of the evaporation depends on the measurement accuracy of short- and long-wave radiation, ground heat and the sensible heat due to wind.

The time variation of the wind velocity also makes the evaluation of the evaporation difficult. Generally evaporation may be evaluated over time scales of hours or days in the field. Therefore, we conducted an evaporation experiment by means of a soil column, filled with Toyoura standard sand (T-soil), under a quasi-unsteady wind velocity by switching high and low speed winds at intervals of Δt (minutes) (Kadono et al. (8)). As a result, the difference in the hourly evaporation flux (HEF) reached a maximum of 12% compared with our previous wind tunnel evaporation experiments, although the hourly averaged wind velocity had the same value for all combinations of high and low speed winds. The soil surface temperature and the wind velocity during the transient period between the high and low speed winds were measured for Chao soil (C-soil) and T-soil in the present wind tunnel evaporation experiments.

This paper describes the characteristics of vapor transfer from the soil surface to the air during the transient period and proposes a new evaporation model to calculate the HEF precisely.

CALCULATION OF EVAPORATION FLUX

Properties of evaporation model

The bulk type equation for water vapor is widely applied to evaluate evaporation flux from the soil surface (Kondo (9)). The evaporation flux, E_v, for the present wind tunnel evaporation experiments can be computed by the following bulk type equation:

$$E_v = \rho C_E \left(q_s - q_{a0}\right) V_{w0} \tag{1}$$

where, E_v = mass evaporation flux (kg/m^2/s); ρ = air density (kg/m^3); C_E = bulk coefficient of evaporation (-); q_s = specific humidity on the soil surface (kg/kg); V_{w0} = free-stream velocity (m/s) (= wind velocity in the free-stream region formed in the outer region of the logarithmic velocity profile, see Fig. 3); and q_{a0} = specific humidity of the air in the free-stream region (kg/kg). It is seen that E_v varies linearly with V_{w0} when C_E and (q_s - q_{a0}) are constant.

E_v (henceforth, evaporation flux) is calculated by Eq. 2 instead of Eq. 1 in this paper.

$$E_v = \alpha_v D_{atm} \left(\rho_{vsurf} - \rho_{vair0}\right) \tag{2}$$

in which α_v = evaporation coefficient (1/m); D_{atm} = diffusion coefficient of vapor in air (m^2/s); ρ_{vsurf} = vapor density on the soil surface (kg/m^3); and ρ_{vair0} = vapor density of the air in the free-stream region (kg/m^3). ρ_{vsurf} is assumed to be the saturated vapor density and is given by a function of the soil surface temperature, T_{surf}, i.e. $\rho_{vsurf}(T_{surf})$. α_v is expressed in terms of V_{w0} (Kadono et al. (8)). The vapor-density difference, (ρ_{vsurf} - ρ_{vair0}), and α_v yield the driving force of the evaporation and the evaporativity due to the movement of air (convection) on the soil surface, respectively.

Hourly evaporation flux (HEF)

Eq. 3 is a conventional model adopted to calculate the HEF, E_{vh1} (kg/m^2/hr),

$$E_{vh1} = 3600(E_v)_{60} \tag{3}$$

The evaporation flux, $(E_v)_{60}$ (kg/m^2/s), is calculated by the following expression of Eq. 4

$$(E_v)_{60} = \alpha_v(V_{w0}^{ave})D_{atm}\{\rho_{vsurf}(T_{surf}^{ave}) - \rho_{vair0}\} \tag{4}$$

The value of α_v is determined from the hourly averaged free-stream velocity, V_{w0}^{ave} (= $(V_{w0}^{high} + V_{w0}^{low})/2$), where V_{w0}^{high} and V_{w0}^{low} are the V_{w0} of high and low speed winds, respectively (see Figs. 2 and 6). ρ_{vsurf} is calculated from the averaged soil surface temperature, T_{surf}^{ave} (=($T_{surf}^{high} + T_{surf}^{low}$)/2), where T_{surf}^{high} and T_{surf}^{low} are the values of T_{surf} in the equilibrium state for V_{w0}^{high} and V_{w0}^{low}, respectively (see Fig. 8).

A new model for calculating the HEF (E_{vh2}) is introduced in this section. E_{vh2} takes into account the nonlinear relation between α_v and V_{w0}, which will be shown in the section "*Evaporation coefficient and evaporation flux*". E_{vh2} can be obtained by summing the cumulative evaporation for all time intervals Δt (minutes) over one hour. That is

$$E_{vh2} = 60\Delta t\sum_{i=1}^{n}(E_{vi})_{\Delta t} \tag{5}$$

in which n represents the switching number of the wind velocity given by $n = 60/\Delta t$.

The evaporation flux, $(E_{vi})_{\Delta t}$ (kg/m^2/s), is denoted by $(E_v)_{\Delta t}^{high}$ and $(E_v)_{\Delta t}^{low}$, which indicate $(E_{vi})_{\Delta t}$ of the high and low speed winds for Δt, respectively.

$$(E_v)_{\Delta t}^{high} = \alpha_v(V_{w0}^{high})D_{atm}\{\rho_{vsurf}(T_{surf}^{high}) - \rho_{vair0}\} \quad \text{for the high speed wind} \tag{6}$$

$$(E_v)_{\Delta t}^{low} = \alpha_v(V_{w0}^{low})D_{atm}\{\rho_{vsurf}(T_{surf}^{low}) - \rho_{vair0}\} \quad \text{for the low speed wind} \tag{6'}$$

The value of α_v is determined individually from V_{w0}^{high} or V_{w0}^{low}, i.e. as $\alpha_v(V_{w0}^{high})$ and $\alpha_v(V_{w0}^{low})$. ρ_{vsurf} is calculated from T_{surf}^{high} or T_{surf}^{low}, respectively.

WIND TUNNEL EVAPORATION EXPERIMENTS

Wind tunnel evaporation experiments were carried out by using a wind tunnel in the National Research Institute

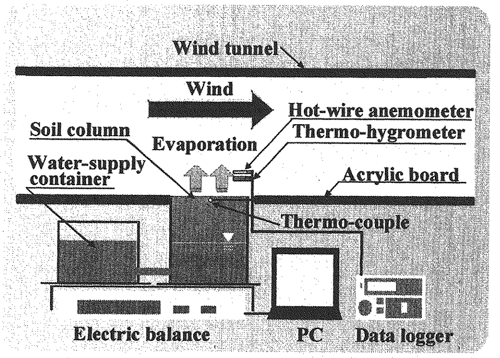

Fig. 1 Experimental equipment

Table 1 Physical properties of soils used in the experiment

Physical properties	Chao soil (C-soil)	Toyoura standard sand (T-soil)
Saturated hydraulic conductivity k_{sat}	9.42×10^{-5} (m/s)	2.04×10^{-2} (m/s)
The average particle diameter D_{50}	0.017 (mm)	0.183 (mm)
Porocity ε	0.40	0.39
Soil classification	Silty clay loam	Sandy soil

for Disaster Prevention. The wind velocity and Δt were automatically controlled from the operator control panel. The present experiment was divided into two wind conditions. The first was a steady evaporation experiment carried out to obtain HEF and the α_v - V_{w0} relation under a single wind velocity. The second was a quasi-unsteady evaporation experiment to obtain HEF under the repetition of high and low speed winds.

Experimental equipment

The wind tunnel evaporation experiment consisted of a wind tunnel (width: 1m, height: 1m, and length: 3m), a soil column (inner diameter: 0.075m and height: 0.08m), an electric balance (minimum reading: 0.01g), a thermo-hygrometer, a hot-wire anemometer and a thermo-couple (see Fig. 1). The bottom of the wind tunnel was covered with acrylic boards.

Table 1 shows the physical properties of C-soil and T-soil used in the experiment, respectively. The C-soil is silty clay loam and its average particle diameter is about one tenth of that of T-soil.

Experimental procedure and conditions

The T-soil and C-soil were packed in a soil column with a dry density of 1600kg/m^3 and 1500kg/m^3, respectively, and then the soil column was filled with water using a water-supply container. The soil column was adjusted so that the soil surface became level with the bottom of the wind tunnel. The air temperature and relative humidity were measured from the soil surface up to a height of 0.4m at intervals of 0.005 to 0.05m and were automatically stored in a computer. T_{surf}^{low} was measured with a thermo-couple inserted 5mm below the soil surface. E_v was measured by means of an electric balance placed under the soil column. The vertical profiles of the air temperature, relative humidity and wind velocity were measured by means of a thermo-hygrometer and a hot-wire anemometer, respectively.

Fig. 2 shows a schematic view of the wind conditions and wind velocities for the quasi-unsteady evaporation experiment. V_{w0}, which was chosen for the steady evaporation experiment, was less than 5.0m/s. Three different combinations of high and low speed winds were designed for the quasi-unsteady evaporation experiment as shown in Table 2. V_{w0}^{low} and V_{w0}^{high} were 0.4 and 5.0m/s for case A, 0.9 and 4.5m/s for case B, and 1.5 and 3.9m/s for case C, respectively. V_{w0}^{ave} of these three cases always had the same value (2.7m/s). The high and low speed winds were automatically changed every 15 or 30 minutes, i.e. Δt = 15 or 30 minutes. The temperature and relative humidity of the ventilated air were controlled within 25 ± 1℃ and 50 ± 3%, respectively.

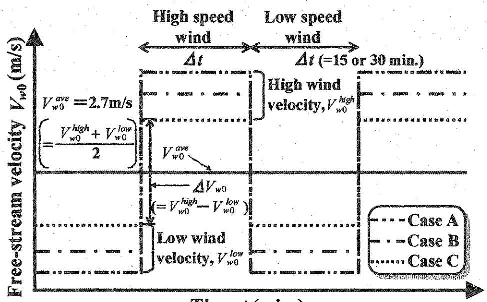

Fig. 2 Schematic view of wind conditions for quasi-unsteady evaporation experiment

Table 2 Experimental wind conditions

Soil	Chao soil and Toyoura standard sand			
Ventilated air	Temperature:25±1℃, Relative humidity:50±3%			
Experimental cases	Free-stream velocity, V_{w0}			
	V_{w0}^{high} (m/s)	V_{w0}^{low} (m/s)	ΔV_{w0} (m/s)	V_{w0}^{ave} (m/s)
Case A	5.0	0.4	4.6	2.7
Case B	4.5	0.9	3.6	2.7
Case C	3.9	1.5	2.4	2.7

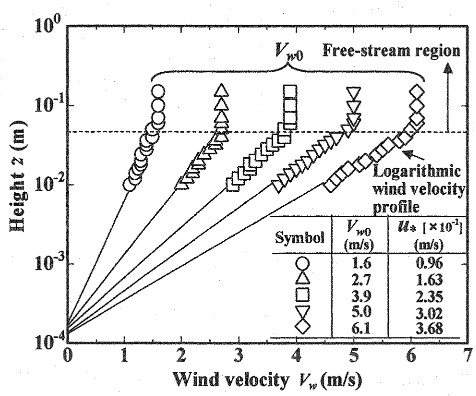

Fig. 3 Vertical profile of wind velocity in the wind tunnel

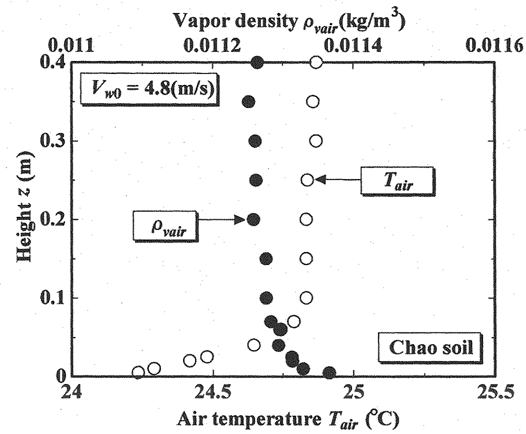

Fig. 4 Vertical profiles of air temperature, T_{air}, and vapor density, ρ_{vair}, in the wind tunnel for V_{w0} = 4.8m/s (C-soil)

EXPERIMENTAL RESULTS

Vertical profile of wind velocity

Fig. 3 shows the vertical profile of the wind velocity in the wind tunnel and V_{w0}. The values of the wall-friction velocity (friction velocity), u_*(m/s), and V_{w0} are also shown in Fig. 3. The logarithmic wind velocity profile expressed by Eq. 7 is valid for $z \leq 0.05$m.

$$\frac{V_w}{u_*} = \frac{1}{\kappa} ln \frac{z}{z_0} \tag{7}$$

in which z_0 = roughness length (m); z = vertical height from the roughness surface (m); V_w = wind velocity at z (m/s) and κ = Karman constant (= 0.4). The average of z_0 was 1.34×10^{-4}m.

Vertical profiles of air temperature and vapor density in the wind tunnel

Fig. 4 shows the vertical profiles of the air temperature, T_{air}, and vapor density, ρ_{vair}, in the wind tunnel for

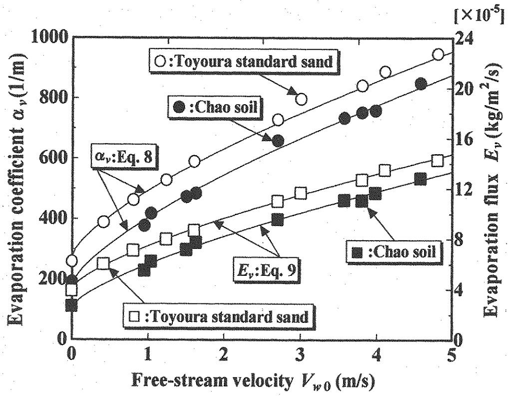

Fig. 5 Evaporation coefficient, α_v, and V_{w0} relation and evaporation flux, E_v, and V_{w0} relation (C-soil and T-soil)

Table 3 Values of the coefficients a, b, c, and d

Coefficient	Chao soil (C-soil)	Toyoura standard sand (T-soil)
a (Eq. 8)	227	221
b (Eq. 8)	178	274
c (Eq. 9)	3.51×10^{-5}	3.49×10^{-5}
d (Eq. 9)	2.51×10^{-5}	3.99×10^{-5}

V_{w0} = 4.8m/s. ρ_{vair} increased toward the soil surface and reached its maximum on the soil surface. On the other hand, T_{air} decreased toward the soil surface and reached its minimum on the soil surface. This profile may be attributed to the latent heat due to evaporation from the soil surface. The boundary layer thickness of T_{air} was almost the same as that of ρ_{vair}. The value of ρ_{vair} for $z \geq 0.1$m was, therefore, adopted as ρ_{vair0} in Eq. 2 and was 1.06×10^{-2}~ 1.15×10^{-2}kg/m^3.

Evaporation coefficient and evaporation flux

Fig. 5 shows the α_v - V_{w0} relation and the E_v - V_{w0} relation obtained from the steady evaporation experiment. The value of α_v decreased for both C-soil and T-soil as V_{w0} became small, but the gradient, $d\alpha_v/dV_{w0}$, became larger as V_{w0} became smaller. The α_v- V_{w0} relation for the two soils is similar to each other and α_v is proportional to the 0.7th power of V_{w0} as expressed by Eq. 8, which is illustrated in Fig. 5.

$$\alpha_v = aV_{w0}^{0.7} + b \tag{8}$$

The coefficients a and b for each soil are shown in Table 3.

The E_v - V_{w0} relation has a similar distribution to the α_v- V_{w0} relation, i.e.

$$E_v = cV_{w0}^{0.7} + d \tag{9}$$

Eq. 9 is shown in Fig. 5 and the coefficients c and d for each soil are shown in Table 3. It is seen that the nonlinearity of Eqs. 8 and 9 is due to appear for V_{w0} < 1.5m/s. As there is no significant difference in (ρ_{vsurf}- ρ_{vair0}) and D_{atm} between all experimental cases, the distribution of the E_v - V_{w0} relation depends mainly on the α_v - V_{w0} relation. Furthermore, it can be inferred that Eq. 1 (linearity of the E_v - V_{w0} relation) is no longer valid, if C_E and (q_s - q_a) are regarded as constants, respectively.

Quasi-unsteady wind velocity and evaporation

Fig. 6 shows the time variation of V_{w0} by changing from high speed wind to low speed wind and vice versa for

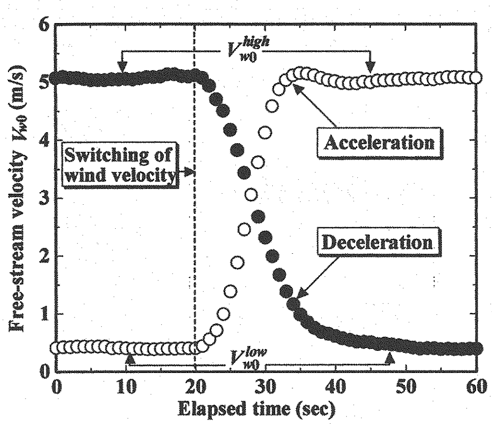

Fig. 6 Time variation of V_{w0} by changing from high speed wind to low speed wind and vice versa (case A)

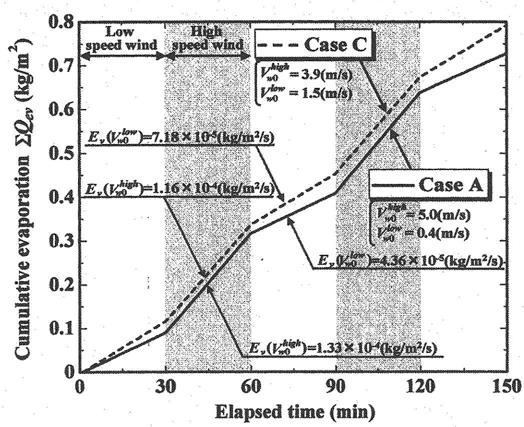

Fig. 7 Time variation of cumulative evaporation by repetition of high and low speed winds (C-soil)

case A. This transition period is termed the recovery period of V_{w0} in this paper. The recovery of V_{w0} was somewhat quicker for acceleration than for deceleration, but both recovery periods were less than 30 seconds.

Fig. 7 shows the time variation of the cumulative evaporation per unit area, ΣQ_{ev} (kg/m^2), for 150 minutes from the beginning of the experiment for the C-soil. ΣQ_{ev} was measured for case A and case C with Δt = 30 minutes. The time gradient of ΣQ_{ev} (= $d\Sigma Q_{ev}/dt = E_v$) was greater for the high speed wind than for the low speed wind. The values of E_v for V_{w0}^{high} and V_{w0}^{low} are shown for case A and case C in Fig. 7. The jag of E_v from the repetition of the high and low speed winds was sharper for case A than for case C, because ΔV_{w0} (= V_{w0}^{high} - V_{w0}^{low}) for case A was greater than that for case C. The difference in ΣQ_{ev} between case A and case C grew with the elapsed time and finally, ΣQ_{ev} of case C was 1.09 times greater than that of case A at 150 minutes of the elapsed time. This difference became especially remarkable during the low speed wind, because the difference in E_v between V_{w0}^{low} = 1.5 and 0.4m/s (for the low speed wind), ΔE_v^{low} (=2.8×10^{-5}kg/m^2/s), is greater than that between V_{w0}^{high} = 5.0 and 3.9m/s (for the high speed wind), ΔE_v^{high} (=1.7×10^{-5}kg/m^2/s), as judged from Fig. 5, although the difference of V_{w0}^{low} (=1.5-0.4) for the low speed wind and the difference of V_{w0}^{high} (= 5.0-3.9) for the high speed wind were the same (1.1m/s).

We also calculated the ratio of E_v for the low and high speed winds, i.e. E_v (V_{w0}^{low} = 1.5m/s) / E_v (V_{w0}^{low} = 0.4m/s) and E_v (V_{w0}^{high} =5.0m/s) / E_v (V_{w0}^{high} =3.9m/s). As a result, the former was 1.64 and the latter was 1.14. Such values were nearly equal to the ratio of α_v for the low and high speed winds, i.e. α_v(V_{w0}^{low} =1.5m/s) / α_v(V_{w0}^{low} =0.4m/s) = 1.61 and α_v(V_{w0}^{high} =5.0m/s) / α_v(V_{w0}^{high} = 3.9m/s) = 1.15, respectively.

Quasi-unsteady soil surface temperature

Attempts were made to examine the mechanism of evaporation of Eq. 2. Fig. 8 shows the time variation of T_{surf} for case A and case C from 30 to 120 minutes after the beginning of the experiment with Δt = 15 minutes. The amplitude of T_{surf}, a_{Tsurf}(= T_{surf}^{low} - T_{surf}^{high}), was greater for case A than for case C. The difference in a_{Tsurf} between case A and case C appeared mainly for the low speed wind, because the difference in T_{surf}^{low} between case A and case C, ΔT_{surf}^{low}, was greater than the difference in T_{surf}^{high} between the two cases, ΔT_{surf}^{high} (See the right edge of Fig. 8). This may be caused by the latent heat flux due to evaporation from the soil surface. The evidence for this assumption was obtained by the foregoing experimental result, $\Delta E_v^{low} > \Delta E_v^{high}$ described in the section "*Quasi-unsteady wind velocity and evaporation*".

Moreover, T_{surf} changed remarkably and immediately after switching the wind velocity and then asymptotically

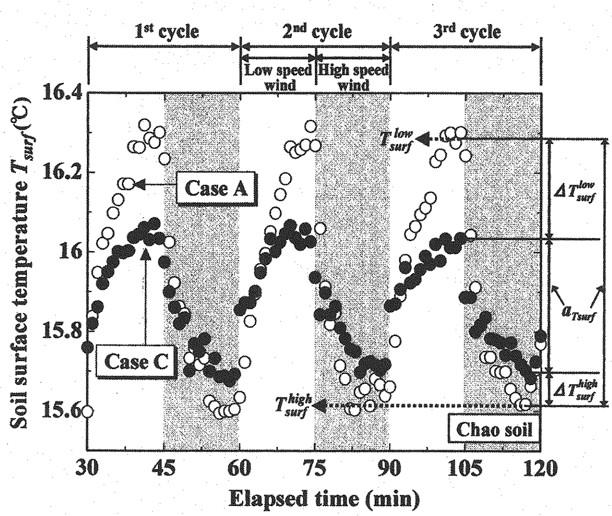

Fig. 8 Time variation of T_{surf} for C-soil from 30 to 120 minutes after beginning of the experiment (case A and case C)

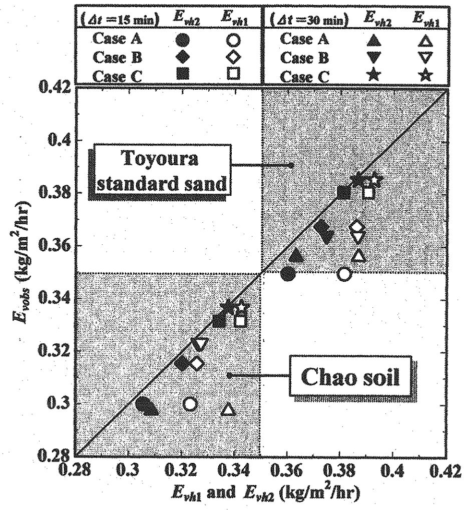

Fig. 9 Comparison of calculated HEF, E_{vh1} and E_{vh2} with observed HEF, E_{vobs}

approached an equilibrium value (T_{surf}^{high} or T_{surf}^{low}), regardless of the acceleration and deceleration (See Fig. 8). The recovery period of T_{surf} is shorter for case C (8 minutes) than for case A (10 minutes). By comparing Figs. 6 and 8, we concluded that the recovery period of T_{surf} is one order smaller than that of V_{w0}.

Comparison of calculated hourly evaporation flux with observed one

Fig. 9 shows the comparison of the two calculated HEF (E_{vh1} (Eq. 3) and E_{vh2} (Eq. 5)) with the observed HEF, E_{vobs}, (= ΣQ_{ev} (at 150 minutes of the elapsed time) $\times 60/150$). The results for $\Delta t = 15$ and 30 minutes are shown together in Fig. 9. E_{vh2} can reproduce E_{vobs} better, compared with E_{vh1} for all experimental cases, regardless of the soil. Eq. 3 always overestimates E_{vobs} and the maximum error between E_{vh1} and E_{vobs} was 8% and 12% for T-soil and for C-soil, respectively. On the other hand, the maximum error between E_{vh2} and E_{vobs} was 3% and 4% for T-soil and for C-soil, respectively. The error regarding E_{vh2} may resulted from neglecting the time variation of V_{w0} or T_{surf} during the recovery period. However, it is clear that E_{vh2} leads to a better prediction than E_{vh1}.

Case A (● and ○, ▲ and △), with large ΔV_{w0} and small V_{w0}^{low} (< 1.0m/s), shows a large difference between E_{vh1} and E_{vh2}. In contrast, when V_{w0}^{low} is greater than 1.5m/s, the difference between E_{vh1} and E_{vh2} becomes small (see the result of case C (■ and □, ★ and ☆)).

As for case B and case C of the C-soil and case A and case C of the T-soil, E_{vobs} for $\Delta t = 30$ minutes was slightly greater than that for $\Delta t = 15$ minutes. However, by taking the experimental accuracy into account, the difference in E_{vobs} described above may be disregarded.

Finally, the overestimation of E_{vh1} may be explained as follows:

E_{vh1} is calculated by inserting Eq. 4 into Eq. 3. That is

$$E_{vh1} = 3600\alpha_v \left(V_{w0}^{ave}\right) D_{atm} \left\{\rho_{vsurf}\left(T_{surf}^{ave}\right) - \rho_{vair0}\right\} \quad (10)$$

On the other hand, the concept of E_{vh2} was in line with the change in E_v associated with V_{w0}. E_{vh2} was, therefore, in good agreement with E_{vobs}. Inserting Eqs. 6 and 6' into Eq. 5 yields the following equation.

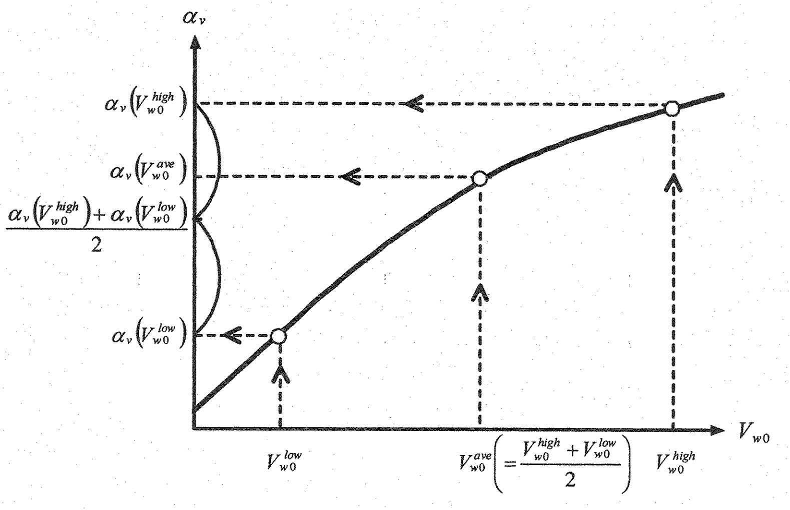

Fig. 10 Schematic view of α_v - V_{w0} relation and difference between $\alpha_v(V_{w0}^{ave})$ and $(\alpha_v(V_{w0}^{high}) + \alpha_v(V_{w0}^{low}))/2$

$$E_{vobs} \approx E_{vh2} = 3600\left[\frac{\alpha_v(V_{w0}^{high})D_{atm}\{\rho_{vsurf}(T_{surf}^{high}) - \rho_{vair0}\} + \alpha_v(V_{w0}^{low})D_{atm}\{\rho_{vsurf}(T_{surf}^{low}) - \rho_{vair0}\}}{2}\right] \quad (11)$$

The following approximation: $\Delta\rho_v = \{\rho_{vsurf}(T_{surf}^{ave}) - \rho_{vair0}\} \approx \{\rho_{vsurf}(T_{surf}^{high}) - \rho_{vair0}\} \approx \{\rho_{vsurf}(T_{surf}^{low}) - \rho_{vair0})\}$ allows Eqs. 10 and 11 can be rewritten as follows:

$$E_{vh1} = 3600\,\alpha_v(V_{w0}^{ave})D_{atm}\Delta\rho_v \quad (12)$$

$$E_{vobs} \approx 3600\,\frac{\alpha_v(V_{w0}^{high}) + \alpha_v(V_{w0}^{low})}{2}D_{atm}\Delta\rho_v \quad (13)$$

Since D_{atm} and $\Delta\rho_v$ in Eqs. 12 and 13 are almost constant, E_{vh1} and E_{vobs} are approximately proportional to $\alpha_v(V_{w0}^{ave})$ and $(\alpha_v(V_{w0}^{high}) + \alpha_v(V_{w0}^{low}))/2$, respectively. That is

$$E_{vh1} \propto \alpha_v(V_{w0}^{ave}) \quad (14)$$

$$E_{vobs} \propto \frac{\alpha_v(V_{w0}^{high}) + \alpha_v(V_{w0}^{low})}{2} \quad (15)$$

Fig. 10 shows a schematic view of the α_v-V_{w0} relation based on Fig. 5. $\alpha_v\,\{\alpha_v(V_{w0}^{high}), \alpha_v(V_{w0}^{low}), \alpha_v(V_{w0}^{ave})\}$ corresponding to three different V_{w0} $\{V_{w0}^{high}, V_{w0}^{low}, V_{w0}^{ave}\}$ are given in Fig. 10. The inequality, $\alpha_v(V_{w0}^{ave}) > (\alpha_v(V_{w0}^{high})+\alpha_v(V_{w0}^{low}))/2$, is obvious. Actually the value of $\alpha_v(V_{w0}^{ave})/\{(\alpha_v(V_{w0}^{high})+\alpha_v(V_{w0}^{low}))/2\}$ is 1.08 for case A of C-soil, and is nearly equal to that of E_{vh1}/E_{vobs} (= 1.10), calculated by Eq. 4. The error included in α_v in Eq. 4 or Eq. 10 can account for the overestimation of the HEF.

CONCLUSIONS

As a first step towards evaluating evaporation under unsteady wind velocities, the time variation of the evaporation flux by switching between high and low speed winds at intervals of 15 or 30 minutes was examined using a wind tunnel. The new evaporation model (Eq. 5) and the conventional model (Eq. 3) were compared with the hourly evaporation flux (HEF) obtained from the wind tunnel evaporation experiments using Chao soil (Silty clay loam) and Toyoura standard sand (Sandy soil).

The conclusions drawn from this study are as follows:

(1) The difference in the HEF exceeded 10% by changing the combinations of the high and low wind velocities, regardless of the soil, although the hourly averaged wind velocity had the same value.

(2) The conclusion (1) was obtained by the nonlinear relation between the evaporation coefficient, α_v, and the free-stream wind velocity, V_{w0}. The nonlinearity of α_v is especially obvious for $V_{w0} \leq 1.5$m/s.

(3) Eq. 1 was no longer valid for the present evaporation experimental results if the bulk coefficient of evaporation, C_E, is constant.

(4) The recovery period of the evaporation flux associated with the change in V_{w0} was affected by the recovery period of the soil surface temperature rather than that of the wind velocity.

(5) The conventional model (Eq. 3) overestimates the observed HEF by 8% and 12% at the maximum for Toyoura standard sand and for Chao soil, respectively. The error of Eq. 3 results from the nonlinearity of the α_v- V_{w0} relation. On the other hand, the new model (Eq. 5) reduced the error of the HEF to between 1/3 and 1/4, compared with that of Eq. 3.

REFERENCES

1. Saito, M. and Yamanaka, T. : Analysis of long-term evapotranspiration data observed by weighing lysimeter and its quality control, Terrestrial Environmental Research Center Papers, Terrestrial Environmental Research Center (TERC), Tsukuba University, No.6, pp.53-62, 2005.
2. Tamagawa, I. : Considerations on the eddy correlation method using sonic anemometer-thirmometer and infrared hygrometer, Journal of Japan Society of Hydrology and Water Resources, Vol.12, No.2, pp.130-138, 1999.
3. Narimatsu, A., Tanaka, K., Morimoto, K. and Takigawa, K. : Direct measurement of surface energy flux over Ariake sea by the eddy correlation method, Coastal Engineering Journal, Vol.52, No.2, pp.1081-1085, 2005.
4. Machimura, T. : Sensible and latent heat flux measurement during rainfall by the eddy correlation method using a fine thermocouple psychrometer, Journal of Agricultural Meteorology, Vol.54, No.4, pp.315-322, 1998.
5. Iwata, T., Toshikawa, K., Nishimura, K., Higuchi, Y., Yamashita, T., Kato, S. and Ohtaki, E. : CO_2 flux measurements over the sea surface by eddy correlation and aerodynamic techniques, Journal of Oceanography, Vol.60, pp.995-1000, 2004.
6. Kondo, J. : A prediction model for the seasonal variation of evaporation from non-vegetated ground surfaces: (1) Model, Journal of Japan Society of Hydrology and Water Resources, Vol.7, No.5, pp.378-385, 1994.
7. Kimura, R., Takayama, N., Kamichika, M. and Matsuoka, N. : Soil water content and heat balance in the loess plateau−Determination of parameters in the three-layered soil model and experimental result of model calculation−, Journal of Agricultural Meteorology, Vol.60, No.1, pp.55-65, 2004.
8. Kadono, K., Fukuhara, T., Terasaki, H., and Nakane, K. : Hourly evaporation flux from soil surface for Toyoura standard sand under quasi-unsteady wind, Proceedings of the 60th annual meeting of Japan Society of Civil Engineers, Vol.60, No.2, pp.55-56, 2005.
9. Kondo, J. : Meteorology of water environment -Heat and water balances on the ground surface-, Asakura publishing Co., Ltd, Japan, pp.108-109, 1994.

APPENDIX – NOTATION

The following symbols are used in this paper:

C_E = bulk coefficient of evaporation (-);

D_{atm} = diffusion coefficient of vapor in air (m^2/s);

E_v = evaporation flux ($kg/m^2/s$);

E_{vh1} = hourly evaporation flux calculated by conventional model ($kg/m^2/hr$);

E_{vh2} = hourly evaporation flux calculated by new model ($kg/m^2/hr$);

$(E_{vi})_{\Delta t}$ = evaporation flux for time interval Δt ($kg/m^2/hr$);

E_{vobs} = observed hourly evaporation flux ($kg/m^2/hr$);

n = switching number of wind velocity per hour;

q_{a0} = specific humidity of air in the free-stream region (kg/kg);

q_s = specific humidity on the soil surface (kg/kg);

T_{surf} = soil surface temperature (℃);

u_* = wall-friction velocity (m/s);

V_w = wind velocity at z (m/s);

V_{w0} = free-stream velocity (m/s);

z = vertical height from roughness surface (m);

z_0 = roughness length (m);

a_v = evaporation coefficient (1/m);

Δt = time interval (min);

$\Delta\rho_v$ = vapor density difference between soil surface and air in the free-stream region (kg/m^3);

κ = Karman constant (= 0.4);

ρ = air density (kg/m^3);

ρ_{vair0} = vapor density of air in the free-stream region (kg/m^3);

ρ_{vsurf} = vapor density on the soil surface (kg/m^3);

Superscript:

ave = averaged;

high = for high speed wind; and

low = for low speed wind.

(Received Jul 31, 2008 ; revised Aug 28, 2009)